Accepted Manuscript

The decisive role played by graphene nanoplatelets on improving the tribological performance of Y_2O_3-Al_2O_3-SiO_2 glass coatings

Alberto Gómez-Gómez, Andrés Nistal, Eugenio García, M. Isabel Osendi, Manuel Belmonte, Pilar Miranzo

PII: S0264-1275(16)31230-8
DOI: doi:10.1016/j.matdes.2016.09.056
Reference: JMADE 2306

To appear in:

Received date: 11 August 2016
Revised date: 14 September 2016
Accepted date: 15 September 2016

Please cite this article as: Alberto Gómez-Gómez, Andrés Nistal, Eugenio García, M. Isabel Osendi, Manuel Belmonte, Pilar Miranzo, The decisive role played by graphene nanoplatelets on improving the tribological performance of Y_2O_3-Al_2O_3-SiO_2 glass coatings, (2016), doi:10.1016/j.matdes.2016.09.056

The decisive role played by graphene nanoplatelets on improving the tribological performance of Y_2O_3-Al_2O_3-SiO_2 glass coatings

Alberto Gómez-Gómez, Andrés Nistal[1], Eugenio García, M. Isabel Osendi, Manuel Belmonte and Pilar Miranzo*

Institute of Ceramics and Glass (ICV-CSIC), Kelsen 5, 28049 Madrid, Spain.

Abstract

Graphene nanoplatelets (GNPs) have proved to be effective fillers for enhancing the mechanical and tribological properties of bulk ceramics and glasses, also with the added benefit of developing electrical and thermal functionalities. Similarly, enhanced transport performance has recently been shown for glass-ceramics coatings of the Y_2O_3-Al_2O_3-SiO_2 (YAS) system containing a small amount of GNP fillers, intended for applications in the aerospace industry. In the present work, the wear and friction behaviour of GNP/YAS coatings –containing 0, 1.2 and 2.3 wt.% GNPs- on silicon carbide substrates is evaluated. The flame spraying process used for coating fabrication induces a structure of splats oriented parallel to the substrate with GNPs located at the inter-splat boundaries forming a connected network of platelets mainly oriented parallel to the surface as well. Unlubricated ball–on-plate reciprocating wear tests show that both the friction coefficient and the wear rate decreased by 35% and 65%, respectively,

[1] Present address: Queen's University Belfast, BT9 5AH, UK

*Corresponding author:
Pilar Miranzo
e-mail: pmiranzo@icv.csic.es

for 2.3 wt% of GNPs. A wear mechanism for GNP/YAS coatings based on both the progressive exfoliation of the graphene sheets and the effect of the GNPs on preventing crack propagation within the coating is proposed.

Keywords. graphene, glass, coatings, thermal spray, wear, friction.

1. Introduction

Different industries often look for materials with increasingly better thermo-mechanical properties at high temperatures to accomplish with requirements of enhanced performance [1-4]. For example, carbon fibre/carbon (C_f/C) and C_f/silicon carbide (C_f/SiC) composites are foreseen as main components of the thermal protection system (TPS) in aerospace launch vehicles, especially in zones that must bear temperatures above 1200 °C during the re-entry into the Earth atmosphere. These state of the art composites should keep good mechanical properties at temperatures above 700 °C, as well as their low weight and small thermal expansion coefficient [5]. However, C_f/C and C_f/SiC composites need to be protected against massive oxidation occurring above 500 °C in atmospheric conditions, which is mainly managed by using ablative coatings [6-8]. In this context, glass-ceramic coatings can provide a proper protection against corrosion and oxidation, while providing self-healing capability at service temperatures. Recently, glass-ceramic coatings with Y_2O_3-Al_2O_3-SiO_2 (YAS) compositions were successfully deposited by flame spraying over SiC, C_f/C and C_f/SiC substrates [9 -11].

On the other hand, common concerns associated to aerospace flights are external perturbations such as ice crystals formation, space debris or micrometeorites impacting the covering tiles during ascent and, therefore, a better tribological performance of the external surfaces would improve the TPS performance. In addition, a reduction of the

friction coefficient (μ) can diminish the heat generated by friction between the ceramic tiles and the atmosphere in the re-entry manoeuvre, decreasing the temperature of the launch fuselage. In this sense, protective coatings containing graphene fillers are expected to reduce the friction and improve the wear performance in a similar way as it was already observed in bulk composites [12-15]. However, there are very few works on the tribological properties of graphene/ceramic composite coatings; in particular, we can mention just the works on zirconia [16] and calcium silicate [17] matrices for bio-medical applications, reporting significant reductions in wear (up to 50%) and friction (29%) in the case of zirconia [16]. To the best of authors' knowledge, there is not any work on the wear properties of glass-ceramic coatings with graphene fillers.

In a previous work by some of the present authors [18] the possibility of achieving YAS hybrid coatings containing graphene nanoplatelets (GNPs) by flame spraying, with enhanced damage tolerance and ablation resistance [19] as well as electrical and thermal functionalities [18], was demonstrated. In present work, the effect of GNPs on the tribological performance of YAS coatings is evaluated by using unlubricated ball-on-plate reciprocating tests at increasing loads. The decisive role of GNPs network within the YAS coating on the wear mechanism is supported by scanning electron microscopy (SEM) observations and micro-Raman spectroscopy analyses.

2. Experimental

The YAS composition in mol.% of 19.2Y_2O_3 (H.C. Starck, Germany)-32.4Al_2O_3 (SM8, Baikowski, France)-48.4SiO_2 (Alfa Aesar, Germany), with a 10 mol. % excess of SiO_2 to counterbalance silica vaporization, was prepared in the same way as described in a previous work [18]. For the GNP/YAS mixtures, high purity (>99.7%) functionalized

GNPs (N008-100-P-10, Angstron Materials Inc., U.S.A.) were used, with x-y dimensions between 5-10 μm and thickness of 50-100 nm. Two different GNP/YAS compositions with 5 and 10 vol.% of GNPs (3.3 and 6.5 wt.%, respectively), were prepared following the same route as described in ref [18]. In short, YAS powders were mixed by attrition milling for 1 h in water; whereas, at the same time, a stable suspension of GNPs (2 $mg \cdot ml^{-1}$) in distilled water was obtained after 30 min of sonication in ultrasonic bath (100 W) by adding 0.4 wt.% of Arabic gum. Subsequently, both GNP and YAS suspensions were mixed and attrition milled for 30 min before freeze drying. Spherical GNP/YAS granules of 30 μm mean size were obtained by spray drying the re-dispersed in water GNP/YAS mixtures (50 wt.% solids content) with 5 wt.% of binder (Optapix PS 94, Zschimmer-Schwarz, Lahnstein, Alemania). SiC plates (Hexoloy S.A., Saint-Gobain, France) were used as substrates, which were grit blasted with SiC particles of ~0.6 mm (Navarro SiC, Spain) for increasing their arithmetical mean roughness (R_a) from 0.2 ± 0.1 to 3.1 ± 0.2 μm. A Si bond coat of ~ 60 μm was previously flame sprayed to assure the mechanical anchoring of the glass-ceramic layer as described elsewhere [20].

The GNP/YAS compositions were flame sprayed onto the Si bond coat with an oxyacetylene gun (CastoDyn DS8000; Eutectic Castolin, Spain) using a gas mixture ratio of 33.3 O_2/27 C_2H_2, in standard litres per minute (SLPM), and a stand-off distance of 14 cm [9, 18]. Weight loss up to 1400 °C of GNP/YAS crushed freestanding coatings were recorded by thermogravimetric analysis (TG, STA 409 Netzsch, Germany) in air at a heating rate of 10 $°C \cdot min^{-1}$ to estimate the actual GNPs content in the coatings, which amounted to 1.2 and 2.3 wt.% for the 3.3 and 6.5 wt.% of GNPs original compositions, respectively. The coatings were correspondingly labelled as YAS-1.2 and YAS-2.3.

Elastic modulus (E) and hardness (H) were evaluated on polished cross-sections of the coatings by instrumented Vickers indentation (ZHU 2.5; Zwick GmbH & Co. KG, Germany), which simultaneously records load and indentation depth. The E parameter of the material was calculated from the reduced modulus using a Poisson coefficient of 0.3. At least seven measurements at a load of 2.9 N were completed for each sample. The indentation imprints were examined by Field Emission Scanning Electron Microscopy (FESEM; S-4700, Hitachi, Japan).

Dry reciprocating ball-on-plate tests were carried out with a UMT-3 tribometer (Bruker Nano Inc., formerly CETR, U.S.A.) to determine μ and the wear volume (W_V) of the GNP/YAS coatings as a function of the applied load and the GNPs content. Both coatings were equally polished reaching final surface roughness $R_a \leq 0.3$ μm for YAS and YAS-1.2 coatings and around 0.8 μm for the YAS-2.3 coating. All tests were performed at 25-30°C and < 25% of relative humidity, using commercial stainless steel 440-C balls (9.5 mm diameter, 62 HRC Rockwell hardness) as counter-bodies. The test parameters were: a stroke length of 2.5 mm, a frequency of 20 Hz and normal applied load (F_N) of 5 N, the total sliding distance (s) being 360 m. At least three tests were performed for each coating composition. Furthermore, for testing the coatings under more severe conditions, the load was increased up to 10 N but the sliding distance was reduced to 150 m; otherwise, the wear track will go through the coating (thickness in the 170-200 μm range). For this load, at least six tests were performed for each type of material.

The μ change with time was on-line registered during testing and the steady state (μ_{ss}) value was estimated by averaging μ data recorded along the sliding distance where stable friction was observed, i.e.160-360 m for the 5 N-360 m tests and 25-150 m for the 10 N-150 m ones. The depth and area of the wear scars were measured with a

profilometer (DEKTAK XT, Bruker, U.S.A.), and the diameter of the wear scars on the tested balls was determined from images of the scanning electron microscope (SEM, Tabletop Microscope TM-1000, Hitachi, Japan). With all these data, the W_V of coatings and balls were calculated, and the corresponding wear rates (W_R) were obtained from the expression $W_R=W_V/(F_N \cdot s)$.

Wear tracks and debris were characterized by FESEM provided with energy-dispersive X-ray spectroscopy (EDS), and also by using confocal Raman spectroscopy (Alpha300 WITec GmbH, Germany). Wear tested areas of 15x15 µm (equivalent to15x15 pixels) were scanned with the laser (532 nm wavelength excitation) using 3 s of acquisition time per spectrum. Quantitative image analyses were done at flat areas appearing on the wear tracks of the GNP/YAS coatings to determine their mean size (d_{50}) and area fraction. At least 500 features were measured on the optical micrographs for each wear track/material pair.

3. Results and Discussion

FESEM observations of the coatings cross-sections (Fig. 1) confirmed that they are continuous, homogeneous and well adhered to the Si bond coat. The thicknesses of the original coatings (YAS and hybrid GNP/YAS) are similar, both being in the 170-200 µm range. The relative density of the coatings, measured by the water immersion technique is also similar, in the range of 76% –80 % of the corresponding theoretical density [18]. The YAS coating (Fig. 1a) is essentially formed by the typical piled-up lamellae, with few spherical pores, attributed to gas entrapped within the low viscosity YAS glass during flame spraying [9]. On the other hand, the GNP/YAS coatings (Fig. 1b,c) show few spherical pores as well but, in contrast, a distinct elongated darker phase

between the flatten lamellae corresponding to the GNPs [18] emerges. The nanoplatelets are plainly noticed protruding from the inter-splat boundaries, as shown in Fig. 1d for the YAS-1.2 coating. The graphene stacks show different thickness and develop also certain corrugation, as they adapt to the lamellae interfaces (see white arrows in Fig. 1d). Sporadically, smaller size GNPs can be seen trapped inside the splats (see black arrows in Fig. 1d).

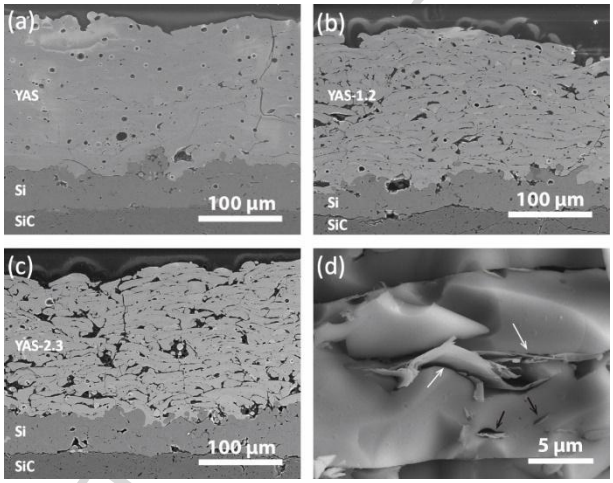

Fig. 1. FESEM micrographs of the polished cross-sections of the (a) YAS, (b) YAS-1.2 and (c) YAS-2.3 coatings. (d) Higher magnification micrograph of the fracture surface of the YAS-1.2 coating, where GNPs can be seen protruding from inter-splat boundaries (pointed by the white arrows). GNPs trapped within a splat are observed in the same image (see black arrows).

The results of the mechanical characterization of these coatings by Vickers indentation tests are summarized in Table 1. H and E data for both hybrid GNP/YAS coatings (~ 4.5 GPa and 70 GPa, respectively) show reductions of about 35% as compared to the YAS plain coating values, which are similar to the decreases reported for bulk composites [21-23]. These decreases of H and E have been linked to a possible week attachment

between the GNPs and the matrix, thus the GNP/YAS interface would become a favourable shearing plane. In the particular case of coatings, a reduction of E is not necessarily detrimental as deformability and strain tolerance would be enhanced.

Table 1. Vickers hardness (H) and elastic modulus (E) of the different coatings.

Coating	**H (GPa)**	**E (GPa)**
YAS	6.7 ± 0.5	110 ± 10
YAS-1.2	4.3 ± 0.5	71 ± 5
YAS-2.3	4.6 ± 0.5	70 ± 10

Fig. 2 reflects μ evolution at 5 and 10 N for the different coatings. At 5 N, there are not (Fig. 2a,b) remarkable differences between μ values of the YAS and YAS-1.2 coatings. Nonetheless, lower μ values are always observed for the YAS-2.3 coating during the first 50 m, although for longer distances, the μ values for the three coatings overlap. Interestingly, at 10 N, friction significantly decreases with the GNPs content for the whole range of the sliding distances. If we look into the behaviour of steady state friction coefficient at 5 N (Fig. 2c), no changes are observed for YAS-1.2 coating whereas for YAS-2.3 coating experiences a slightly decrease. Nevertheless, at higher loads (10 N), the constant decay of μ_{ss} with the GNPs content is evident, reaching 35 % reduction in μ_{ss} for the YAS-2.3 coating as compared to the blank coating.

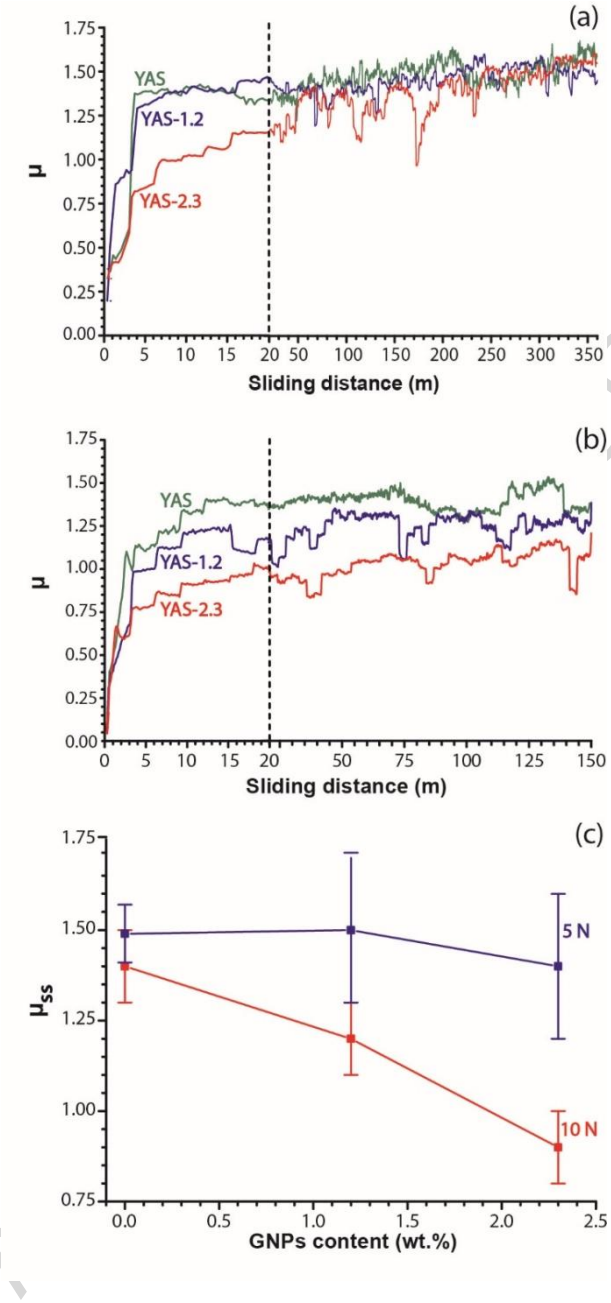

Fig. 2. Friction coefficient (μ) evolution with the sliding distance during the reciprocating sliding tests at (a) 5 and (b) 10 N. (c) Steady state friction coefficient (μ_{ss}) values as a function of the GNPs content at the two tested loads.

As it can be seen in Fig. 3a,b, the wear volume decreases when adding GNPs and this reduction is again more prominent for the higher load tests. Actually, W_V for

YAS-1.2 and YAS-2.3 coatings decreased at 5 N by 40% and 20%, respectively, as compared to the YAS coating, whereas at 10 N reductions were correspondingly of 45% and 65%. In a similar way, the W_R at 5 N (Fig. 3c) fluctuates in the range 1.0-1.7 $\times 10^{-4}$ $mm^3 \cdot N^{-1} \cdot m^{-1}$ for all coatings, but being always slightly lower for the hybrid coatings than for plain YAS. Conversely, W_R at 10 N abruptly decreases with the GNPs content, diminishing by ≈65% for YAS-2.3 coating (Fig. 3c). The range of W_R values (in the order of 10^4 mm^3 N^{-1} m^{-1}) indicates that severe wear regime prevailed in all cases (i.e., coatings and testing conditions) however the dominant wear mechanism depended on whether or not the coating contained GNPs.

On the other hand, it was quite remarkable that W_V of the steel balls were rather low (0.15 - 0.20 mm^3) and no substantial changes with load were measured in the case of the hybrid coatings. For the case of the hybrid YAS-2.3 coating, lower wear volumes values were attained at 10 N than at 5 N (Fig. 3b), results that again support the active role of the GNPs in the wear process for high test loads.

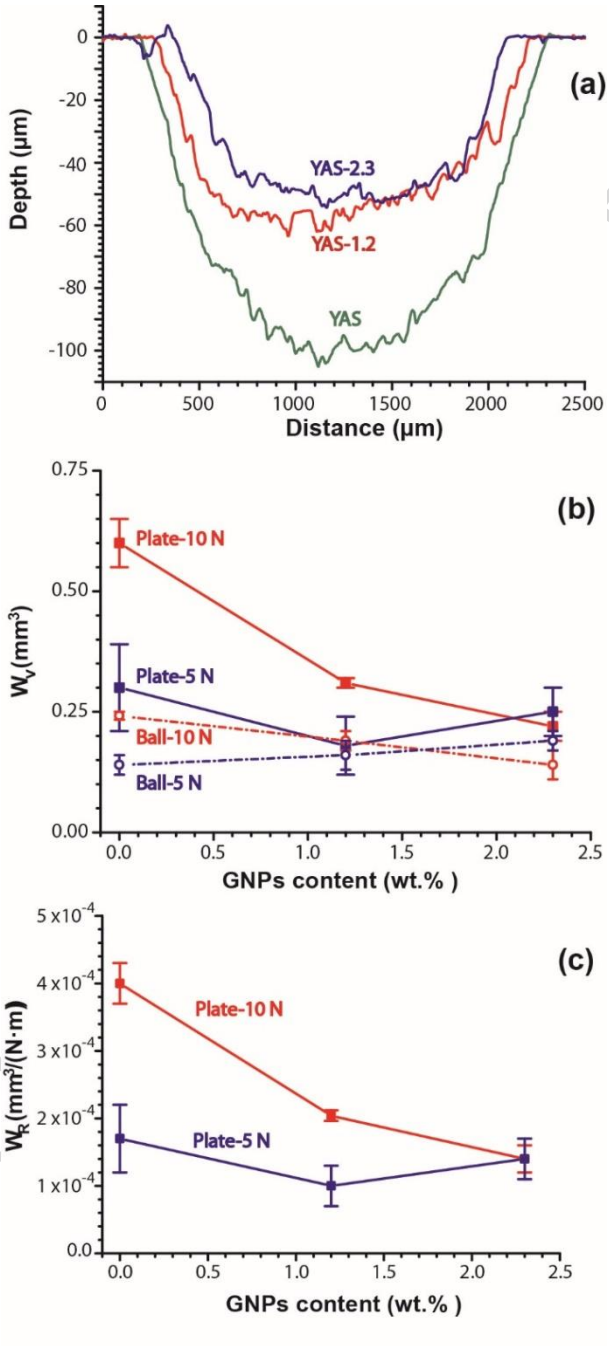

Fig. 3. (a) 2D profiles of representative wear tracks of the different coatings tested at 10 N; (b) Wear volume (W_V) versus GNPs content of the plates (coatings) and the balls tested at 5 and 10 N; and (c) wear rate (W_R) versus GNPs content of the coatings tested at 5 and 10 N.

FESEM observations of the wear scars on the coatings (Fig. 4) confirm that different wear processes are operative for each material type. For the plain YAS coating, a rough

scar linked to the formation of a tribofilm – displaying a higher compaction at 10 N than at 5 N- is clearly observed. This tribofilm appears extremely cracked probably because of the intense cyclic fatigue of the surface and the rising of internal stresses. The large W_V of the YAS coating is then explained by the typical brittle behaviour of glass coatings –as the development of long radial cracks emanating from the corners of indentation prints infers (Fig. 5a)–, which most probably produces the instability of the generated debris.

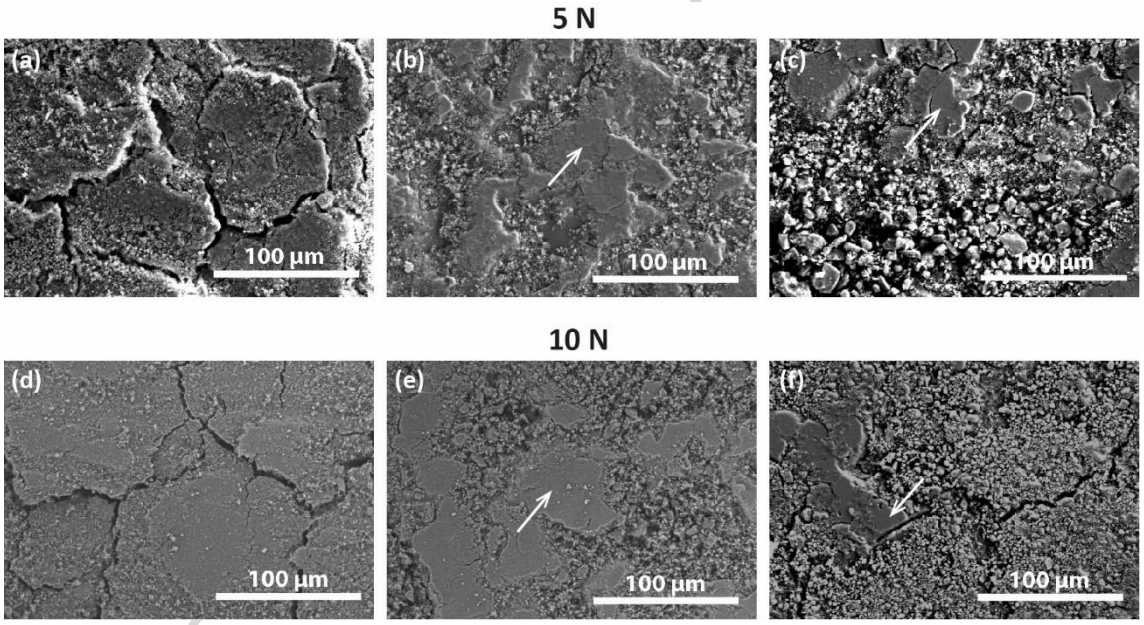

Fig. 4. SEM micrographs of the surfaces tested at 5 and 10 N for the different coatings: YAS (a,d), YAS-1.2 (b,e), and YAS-2.3 (c,f). Arrows point to the generated plateau-like areas that are surrounded by powdered debris.

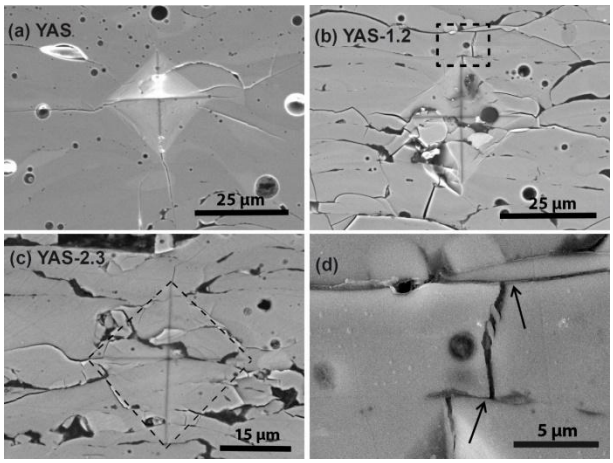

Fig. 5. FESEM micrographs showing Vickers indentation prints performed at 2.9 N on the polished cross sections of the YAS (a), YAS-1.2 (b) and YAS-2.3 (c) coatings. (d) High magnification image of the boxed area in (b) showing an indentation crack deflected by the graphene nanoplatelets located at inter-splat locations (see black arrows).

Conversely, the wear tracks of the YAS-1.2 and YAS-2.3 coatings show two types of features, plateau-like areas and crushed debris surrounding them (Fig. 4), each with a clearly distinct morphology. These plateaus are perceived as brighter features in the optical images of the wear tracks shown in Fig. 6. The area fraction of plateaus, quantified by image analysis, is higher for the YAS-2.3 coating (0.20 for both loads) than for the YAS-1.2 (0.09 and 0.08 for 5 and 10 N, respectively), and their average size decreases when increasing load, especially for the YAS-2.3 coating – from 30 to 25 µm in YAS 1.2, and from 62 to 40 µm in YAS-2.3.

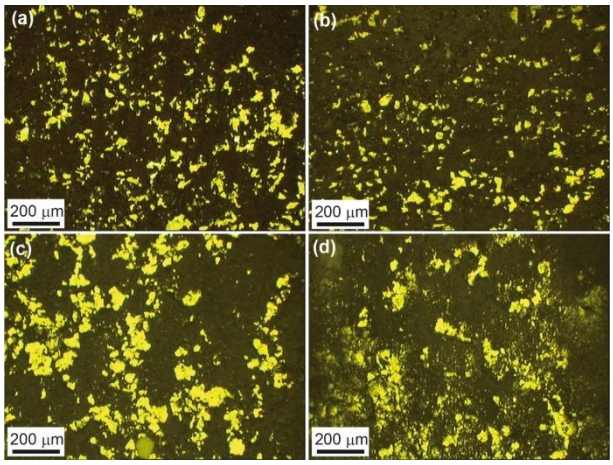

Fig. 6. Optical images of the wear tracks for the YAS-1.2 coating at 5 N (a) and 10 N (b), and the YAS-2.3 coating at 5 N (c) and 10 N (d).

The EDS analysis of the plateaus observed on the wear tracks for the hybrid GNP/YAS coatings (Fig. 7a,c) confirm the presence of atomic elements from the YAS matrix (Si, Al and Y) as well as some carbon content (probably coming from the GNPs). The micro-Raman spectra of the carbon rich areas on the plateaus (also included in Fig. 7b,d) verified the presence of some GNPs, also showing a slight increase in the intensity ratio between the D- and G- characteristic bands of graphene compared to the untested coating (0.36 versus 0.64 for the YAS-2.3 coating tested at 10 N). Therefore, these flat regions would correspond to splats in which some GNPs still remain attached.

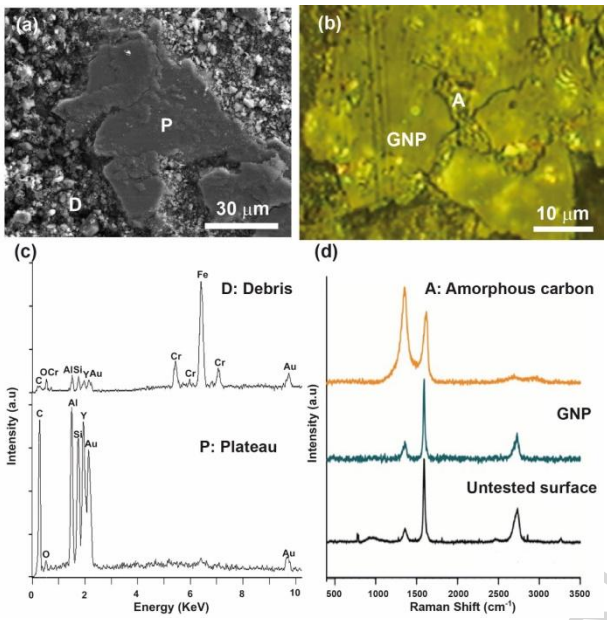

Fig. 7. (a) SEM micrograph of the YAS-2.3 hybrid coating tested at 5 N showing a typical plateau (P) surrounded by powdered debris (D). (b) Optical image of one of these flat regions. (c) EDS recorded from the areas marked with D and P in (a). (d) Representative micro-Raman spectra corresponding to damaged GNPs–marked with A in (b)– showing an amorphous carbon-like spectrum, undamaged GNPs and the original untested coating surface.

The worn zone in Fig 7a (D in the image) and the corresponding microanalysis shown in Fig. 7c indicate that the powdered material contains elements from both the coating and the ball, and the micro-Raman spectrum of a similar zone (marked with an A in Fig. 7d) shows the typical bands of amorphous carbon, where 2D band has completely disappeared and the D-band associated to the presence of defects is more intense and wide that the G band (I_D/I_G ~ 2.05). The defective nature of carbon species in the debris indicates the occurrence of intense damage of GNPs during the sliding process. Therefore, although the hybrid coatings also exhibit a severe wear process, the

presence of flat islands related to splats with adhered GNPs and surrounded by crushed debris implies a wear mechanism based on the progressive exfoliation of the multilayer graphene previous to the crushing of splats and GNPs flakes, which retards matter removal. This mechanism is compatible with previous results on bulk GNP/ceramic composites reported by some of the present authors [13,15], where the exfoliation of the nanoplatelets and their incorporation to an adherent protective tribofilm have been observed in two different types of materials and wear tests, i.e. isooctane lubricated conditions- GNP/Si_3N_4 composites with addition of 3 wt.% GNP [13]- and unlubricated conditions –GNP/SiC composites with 5 - 20 vol.% GNP [15].

The proposed mechanism is expected to become more effective with increasing GNPs content and loads. Average Raman spectra recorded for both hybrid coatings on plateau areas of 15 x 15 μm (Fig. 8) agree with this statement. In spite of the larger area of flat regions present in the wear scars of the YAS-2.3 coating (Fig. 6) -20 versus 9 % in the YAS-1.2 coating-, the Raman intensity of the three different bands of graphene are similar for both coatings tested at 5 N, with I_D/I_G in the range of 1.4-1.6, which is significantly higher than that observed for GNPs on the untested surface. This fact would mean that graphene flakes equally contribute to the wear/friction process at 5 N in the hybrid coatings, explaining the very similar values obtained for both materials.

On the other hand, at 10 N, the average size of the flat regions significantly decreases, especially for the YAS-2.3 coating (35% lower). The Raman analysis of the YAS-1.2 coating shows that the I_D/I_G ratio drastically increases reaching values of ~ 2.0 and the 2D-band almost vanishes, which are indications that most of the carbon becomes amorphous. Accordingly, the increasingly active role of graphene with load in this tribological system is fully revealed. In the case of the YAS-2.3 coating, the I_D/I_G

value (1.4) did not change with the load, which also points to a potential ability of this coating to improve wear response at even higher loads.

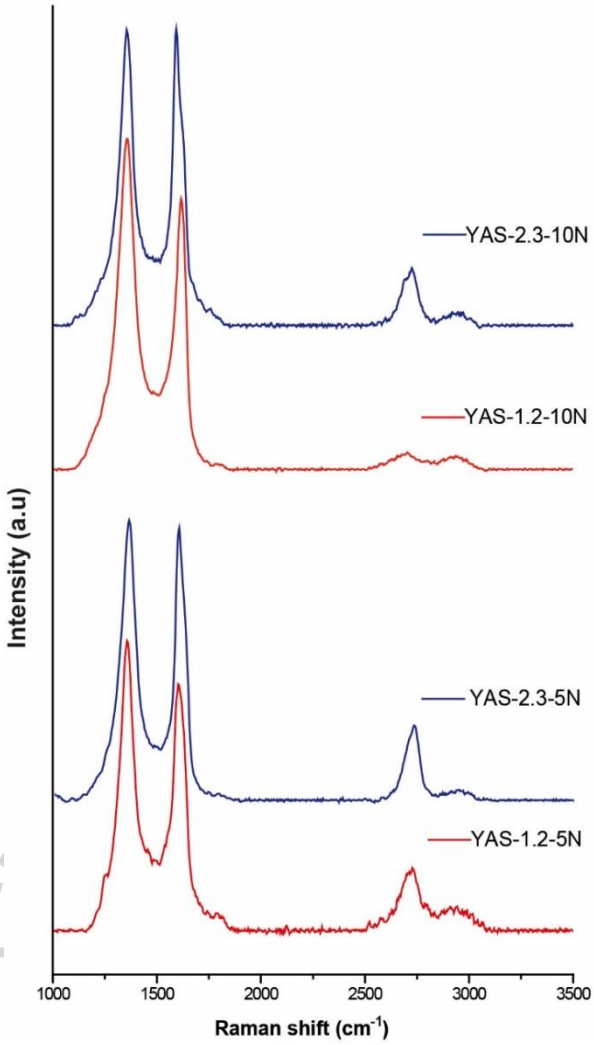

Fig. 8. Average micro-Raman spectra recorded on 15x15 µm areas of plateaus like those shown in Fig. 6 for the YAS-1.2 and YAS-2.3 coatings at 5 N and 10 N.

Moreover, the proposed wear mechanism is also congruent with the mechanical properties of the GNP/YAS coatings. As it is shown in Fig. 5b,c, the indentation damage in the case of the hybrid coatings is linked to a favourable shearing along the weak inter-splat boundaries where graphene sheets are situated. Besides, the

propagation of radial cracks emanating from the indentation corners, which were typically generated in the brittle YAS coating (Fig. 5a), is limited in the case of the GNP/YAS coatings (Fig. 5b,c). This mechanical behaviour is compatible with an increased toughness and damage resistance dominated by frictional dissipation at sliding interfaces. In fact, when indentation median cracks generated at the imprint corners in the hybrid coatings propagate (see black arrows in Fig. 5d), they were either arrested or bridged by GNPs at inter-splat locations. These phenomena are promoted in the direction perpendicular to the GNP basal plane –i.e. to the coating surface- and then wear damage inside the hybrid coatings is prevented, whereas exfoliation of the GNPs is favoured helping lubrication. Both aspects would explain the improved wear resistance and lower friction coefficient of these hybrid coatings with increasing load and GNPs amount. Fig. 9 shows the schematic explaining the wear scar evolution for the plain YAS and hybrid GNP/YAS coatings associated to the proposed mechanism. Crack arresting by GNPs in the direction perpendicular to the surface and GNPs pull-out and exfoliation are portrayed for the GNP/YAS coating. Conversely, cracks propagation and coalesce along the inter-splat boundaries leading to extended damage are the leading features in YAS coating.

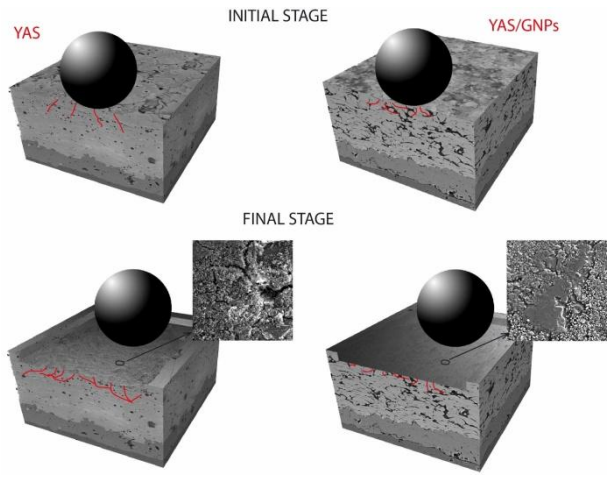

Fig. 9. Schematic of the wear scars evolution for the plain YAS and the hybrid GNP/YAS coatings. Crack arresting by GNPs is promoted in the direction perpendicular to the surface for the hybrid coating, limiting inner wear damage, whereas exfoliation of the GNPs over plateaus is favoured. Conversely, cracks propagate along the inter-splat boundaries and coalesce leading to extended damage in the YAS coating.

4. Conclusions

The incorporation of small amounts –up to 2.3 wt.%- of GNPs as fillers for Y_2O_3-Al_2O_3-SiO_2 glass coatings is proved effective for enhancing their tribological properties. The coating structure developed by the flame spraying process, consisting of GNPs preferentially located at the inter-splat boundaries and oriented parallel to the substrate surface, appears determinant for explaining the wear mechanism. Under severe wear conditions, both the friction coefficient and the wear volume decrease as GNPs content increases. These reductions are consistently larger (around 35% and 65% for μ and W_R, respectively) when increasing the applied load from 5 to 10 N. A wear mechanism for the GNP/YAS hybrid coatings is proposed based on the progressive exfoliation of the graphene before the crushing of splats and GNPs flakes -thus retarding matter removal. The anisotropic mechanical properties of the hybrid coatings, due to the orientation of the GNPs parallel to the coating surface, induces the crack arrest in the direction perpendicular to the surface, limiting wear damage inward. Besides, exfoliation of the GNPs is favoured helping the lubrication of the tribosystem.

Acknowledgments

This work was supported by the Spanish Ministry of Economy and Competitiveness (MINECO) and the FEDER program under project IPT-2012-0800-420000 and by CSIC under project 201360E063.

References

[1] W. Krenkel, F. Berndt, C/C−SiC Composites for Space Applications and Advanced Friction Systems, Mater. Sci. Eng. A, 412 (2005), 177−181.

[2] F. Christine, Design, Fabrication and Application of Thermostructural Composites (TSC) like C/C, C/SiC, and SiC/SiC Composites, Adv. Eng. Mat., 4 (2002), 903-912.

[3] I. Spitsberg, J. Steibel, Thermal and Environmental Barrier Coatings for SiC/SiC CMCs in Aircraft Engine Applications, Int. J. Appl. Ceram. Technol., 1 (2004), 291−301.

[4] B. Behrens, M. Muller, Technologies for Thermal Protection Systems Applied on Re-usable Launcher, Acta Astronaut., 55 (2004), 529-536.

[5] K. K. Chawla, Ceramic Matrix Composites, Chapman and Hall, London, 1993

[6] J.N. Stuecker, D.A. Hirschfeld, D.S. Martin, Oxidation protection of carbon–carbon composites by sol–gel ceramic coatings, J. Mater. Sci., 34 (1999), 5443–5447.

[7] K.A. Weidenmann, G. Rixecker, F. Aldinger, Liquid phase sintered silicon carbide (LPS–SiC) ceramics having remarkably high oxidation resistance in wet air, J. Eur. Ceram. Soc., 26 (2006), 2453–2457.

[8] L.M. Manocha, S.M. Manocha, Studies on solution-derived ceramic coatings for oxidation protection of carbon–carbon composites, Carbon, 33 (1995), 435–440.

[9] E. García, A. Nistal, F. Martín de la Escalera, A. Khalifa, M.A. Sainz, M.I. Osendi, P. Miranzo, Thermally sprayed Y_2O_3-Al_2O_3-SiO_2 coatings for high temperature protection of SiC ceramics, J. Therm. Spray Technol., 24 (2015), 185−193.

[10] C. Marraco-Borderas, A. Nistal, E. García, M.A. Sainz, F. Martín de la Escalera, Y. Essa, P. Miranzo, Adhesion of Y_2O_3-Al_2O_3-SiO_2 coatings to typical aerospace substrates, Bol. Soc. Esp. Ceram. Vidrio, 55 (2016), 127-135. doi:10.1016/j.bsecv.2016.01.005.

[11] M. A. Sainz, M. I. Osendi, P. Miranzo, Protective Si–Al–O–Y glass coatings on stainless steel in situ prepared by combustion flame spraying, Surf. Coat. Technol. 202 (2008), 1712-1717.

[12] P. Hvizdoš, J. Dusza, C. Balázsi, Tribological properties of Si_3N_4–graphene nanocomposites, J. Eur. Ceram. Soc., 33 (2013), 2359–2364.

[13] M. Belmonte, C. Ramirez, J. Gonzalez-Julian, J. Schneider, P. Miranzo, M.I. Osendi, The beneficial effect of graphene nanofillers on the tribological performance of ceramics, Carbon, 61 (2013), 431–435.

[14] H. J. Kim, S. M. Lee, Y. S. Oh, Y. H. Yang, Y. S. Lim, D. H. Yoon, C. Lee, J.Y. Kim, R.S. Ruoff, Unoxidized graphene/alumina nanocomposite: fracture-and wear-resistance effects of graphene on alumina matrix, Sci. Rep., 4 (2014), 5176.

[15] J. Llorente, B. Román-Manso, P. Miranzo, M. Belmonte, Tribological performance under dry sliding conditions of graphene/silicon carbide composites. J. Eur. Ceram. Soc., 36 (2016), 429-435.

[16] H. Li, Y. Xie, K. Li, L. Huang, S. Huang, B. Zhao, X. Zheng, Microstructure and wear behavior of graphene nano-sheets-reinforced zirconia coating, Ceram. Int., 40 (2014), 12821-12829.

[17] Y. Xie, H. Li, C. Zhang, X. Gu, X. Zheng, L Huang, Graphene-reinforced calcium silicate coatings for load-bearing implants, Biomed. Mater. 9 (2014), 025009 (7pp)

[18] E. García, A. Nistal, A. Khalifa, Y. Essa, F. Martín de la Escalera, M.I. Osendi, P. Miranzo, Highly Electrically Conducting Glass-Graphene Nanoplatelets Hybrid Coatings, ACS Appl. Mater. Interfaces, 7 (2015), 17656−17662.

[19] E. García, A. Nistal, M.I. Osendi, P. Miranzo, Superior performance of ablative glass coatings containing graphene nanosheets, J. Am. Ceram. Soc. (2016), in press, DOI: 10.1111/jace.14447.

[20] A. Nistal, E. García, C. García-Diego, M.I. Osendi, P. Miranzo, Flame Spraying of Adherent Si Coatings on SiC Substrates, Surf. Coat. Technol., 270 (2015), 8−15.

[21] C. Ramirez, P. Miranzo, M. Belmonte, M.I. Osendi, P. Poza, S.M. Vergara-Díaz, M. Terrones, Extraordinary toughening enhancement and flexural strength in Si3N4 composites using graphene sheets, J. Eur. Ceram. Soc., 34 (2014), 161-169

[22] H. Porwal, P. Tatarko, S. Grasso, C. Hu, A.R. Boccaccini, I. Dlouhý, M.J. Reece, Toughened and machinable glass matrix composites reinforced with graphene and graphene-oxide nanoplatelets, Sci. Technol. Adv. Mater., 14 (2013), 055007 (10pp).

[23] M. Belmonte, A. Nistal, P. Boutbien, B. Román-Manso, M.I. Osendi, P. Miranzo, Toughened and strengthened silicon carbide ceramics by adding graphene-based fillers, Scripta Mater., 113 (2016), 127-130.

Captions

Fig. 1. FESEM micrographs of the polished cross-sections of the (a) YAS, (b) YAS-1.2 and (c) YAS-2.3 coatings. (d) Higher magnification micrograph of the fracture surface of the YAS-1.2 coating, where GNPs can be seen protruding from inter-splat boundaries (pointed by the white arrows). GNPs trapped within a splat are observed in the same image (see black arrows).

Fig. 2. Friction coefficient (μ) evolution with the sliding distance during the reciprocating sliding tests at (a) 5 and (b) 10 N. (c) Steady state friction coefficient (μ_{ss}) values as a function of the GNPs content at the two tested loads.

Fig. 3. (a) 2D profiles of representative wear tracks of the different coatings tested at 10 N; (b) Wear volume (W_V) versus GNPs content of the plates (coatings) and the balls tested at 5 and 10 N; and (c) wear rate (W_R) versus GNPs content of the coatings tested at 5 and 10 N.

Fig. 4. SEM micrographs of the surfaces tested at 5 and 10 N for the different coatings: YAS (a,d), YAS-1.2 (b,e), and YAS-2.3 (c,f). Arrows point to the generated plateau-like areas that are surrounded by powdered debris.

Fig. 5. FESEM micrographs showing Vickers indentation prints performed at 2.9 N on the polished cross sections of the YAS (a), YAS-1.2 (b) and YAS-2.3 (c) coatings. (d) High magnification image of the boxed area in (b) showing an indentation crack deflected by the graphene nanoplatelets located at inter-splat locations (see black arrows).

Fig. 6. Optical images of the wear tracks for the YAS-1.2 coating at 5 N (a) and 10 N (b), and the YAS-2.3 coating at 5 N (c) and 10 N (d).

Fig. 7. (a) SEM micrograph of the YAS-2.3 hybrid coating tested at 5 N showing a typical plateau (P) surrounded by powdered debris (D). (b) Optical image of one of these flat regions. (c) EDS recorded from the areas marked with D and P in (a). (d) Representative micro-Raman spectra corresponding to damaged GNPs–marked with A in (b)– showing an amorphous carbon-like spectrum, undamaged GNPs and the original untested coating surface.

Fig. 8. Average micro-Raman spectra recorded on 15x15 μm areas of plateaus like those shown in Fig. 6 for the YAS-1.2 and YAS-2.3 coatings at 5 N and 10 N.

Fig. 9. Schematic of the wear scars evolution for the plain YAS and the hybrid GNP/YAS coatings. Crack arresting by GNPs is promoted in the direction perpendicular to the surface for the hybrid coating, limiting inner wear damage, whereas exfoliation of the GNPs over plateaus is favoured. Conversely, cracks propagate along the inter-splat boundaries and coalesce leading to extended damage in the YAS coating.

Graphical abstract

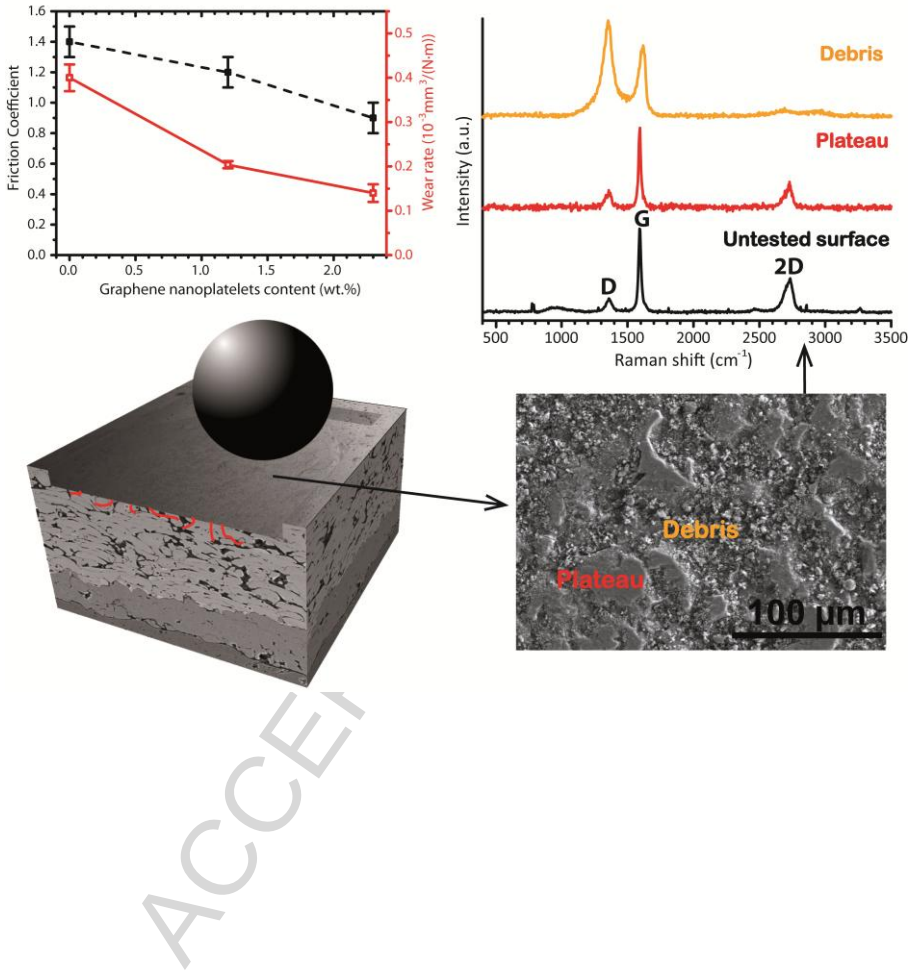

Highlights

- Graphene flakes located at inter-splat boundaries have a decisive role on the tribological performance of flame sprayed graphene/glass coatings.
- The favourable effect of graphene clearly manifests at higher test loads; friction coefficient and wear rate decreasing with graphene content.
- The friction coefficient of the coatings reduces by 35% with just 2.3 wt.% of graphene nanoplatelets.
- Wear rate decreases up to 65% for the coating with 2.3 wt % of graphene flakes.
- The enhanced performance is attributed to the progressive exfoliation of graphene stacks and their incorporation to debris as lubricant.